AMERICAN SOCIETY of
GENE & CELL
THERAPY

Efficient Delivery and Nuclear Uptake Is Not Sufficient to Detect Gene Editing in CD34+ Cells Directed by a Ribonucleoprotein Complex

Shirin R. Modarai,[1,4] Dula Man,[1,4] Pawel Bialk,[1] Natalia Rivera-Torres,[2] Kevin Bloh,[3] and Eric B. Kmiec[1]

[1]Gene Editing Institute, Helen F. Graham Cancer Center, Newark, DE 19713, USA; [2]Department of Medical Sciences University of Delaware, Newark, DE 19716, USA; [3]Nemours Center for Childhood Cancer Research, Alfred I. duPont Hospital for Children, Wilmington, DE 19803, USA

CD34+ cells are prime targets for therapeutic strategies for gene editing, because modified progenitor cells have the capacity to differentiate through an erythropoietic lineage. Although experimental advances have been reported, the associated experimental protocols have largely been less than clear or robust. As such, we evaluated the relationships among cellular delivery; nuclear uptake, often viewed as the benchmark metric of successful gene editing; and single base repair. We took a combinatorial approach using single-stranded oligonucleotide and a CRISPR/Cas9 ribonucleoprotein to convert wild-type HBB into the sickle cell genotype by evaluating conditions for two common delivery strategies of gene editing tools into CD34+ cells. Confocal microscopy data show that the CRISPR/Cas9 ribonucleoprotein tends to accumulate at the outer membrane of the CD34+ cell nucleus when the Neon Transfection System is employed, while the ribonucleoproteins do pass into the cell nucleus when nucleofection is used. Despite the high efficiency of cellular transformation, and the traditional view of success in efficient nuclear uptake, neither delivery methodology enabled gene editing activity. Our results indicate that more stringent criteria must be established to facilitate the clinical translation and scientific robustness of gene editing for sickle cell disease.

INTRODUCTION

Sickle cell disease (SCD) arises primarily from a genetic mutation occurring in the third position of the sixth codon of the human β-globin gene. This universal mutation has been the focus of work by investigators interested in developing gene therapy approaches to this inherited disease. Clearly, other changes in the genomes of individual patients can modulate both penetrance and responsiveness to traditional therapy. However, it is generally recognized that reversing this mutation within the context of the chromosome would bring substantial improvement in the health and quality of life of the SC patient. With the advancement of genetic engineering and genome editing technologies, it is possible to envision a genetic remedy for the sickle cell mutation. In our laboratory, we are focused on single-stranded oligonucleotides (ssODNs) as effector molecules to direct the correction of single base mutations. Although successful application of single-agent gene editing has been demonstrated in proof-of-principle experiments,[1] the frequency with which the mutation is repaired or reversed falls below clinically relevant levels.

In an effort to increase the frequency of gene repair through nucleotide exchange, the combinatorial approach uniting ssODNs and CRISPR/Cas9 has begun to emerge as a feasible therapeutic approach. Dever et al.[2] reported efficient CRISPR/Cas9 gene editing at the β-globin locus in hematopoietic stem cells using a Cas9 ribonucleoprotein (RNP) and an adeno-associated viral vector to deliver the donor DNA sequence. Earlier studies had demonstrated efficient targeting through the combination of zinc-finger nucleases and ssODNs or similarly structured donor DNA delivered by lentiviral vectors. Xu et al.[3] showed that CRISPR/Cas9 gene editing can be used to correct a consensus T mutation important in the development of thalassemia by using a mechanism in which a donor fragment containing HBB intron 2 is inserted via homologous recombination at the proper site and at a relevant frequency. These two studies use a combination of transposition, physical delivery through Neon transformation or nucleofection, and viral delivery, in some cases, to introduce the proper gene editing tools into progenitor cells. A robust and consensus delivery strategy that can guide investigators interested in studying the mechanism of CRISPR/Cas9 uptake and its subsequent action is lacking. To address this issue, Hendriks et al.[4] proposed using lipid-based transfection for the delivery of CRISPR/Cas9 for gene correction, but delivery of gene editing tools in primary cell cultures remains problematic. Some studies outline mechanisms and formats for delivering gene editing tools, but none of them provide a primary quantitative analysis of efficiency of delivery.[5-7] The experimental readout is simply an indirect measure of gene editing activity that, in some cases, could be unrelated to the efficiency of vehicle transfection. The protocols and mode of vehicle delivery used for gene editing are often described with minimal detail that

Correspondence: Eric B. Kmiec, Gene Editing Institute, Center for Translational Cancer Research, Helen F. Graham Cancer Center & Research Institute, Christiana Care Health System, 4701 Ogletown-Stanton Road, Suite 4300, Newark, DE 19713, USA.
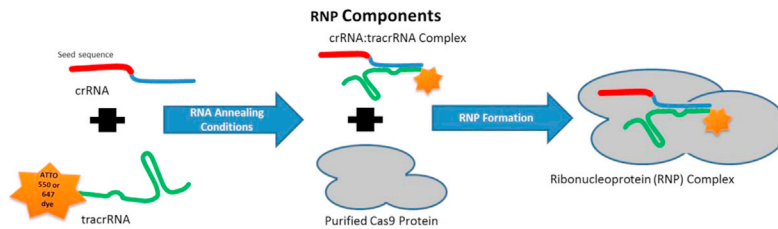**E-mail:** eric.b.kmiec@christianacare.org

A

Mutant eGFP gene sequence:

5' TCTGCACCACCGGCAAGCTGCCCGTGCCCTGGCCCACCCTCGTGACCACCCTGACCTA**G**GGCGTGCAGTGCTTCAGCCGCTACCCCGACCACATGAAGCAGCACGACTTCTT '3 NT
3' AGACGTGGTGGCCGTTCGACGGGCACGGGACCGGGTGGGAGCACTGGT**GGA**C**T**GGATC**C**CGCACGTCACGAAGTCGGCGATGGGGCTGGTGTACTTCGTCGTGCTGAAGAA '5 T
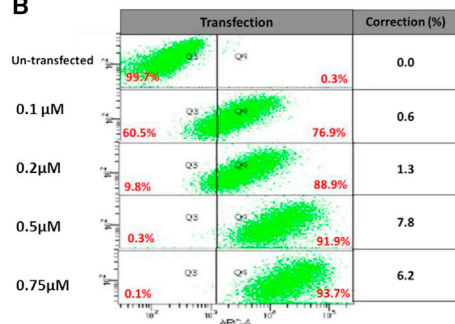
2C

180mer(NT):

3' A*C*G*GTGGATGCCGTTCGACTGGGACTTCAAGTAGACGTGGTGGCCGTTCGACGGGCACGGGACCGGGTGGGAGCACTGGTGGGACTGG**AT**GCCGCACGTCACGAAGTCGGCGATGGGGCTGGTGTACTTCGTCGTGCTGAAGAAGTTCAGGCGGTACGGGCTTCCGATGCAGGTCCT*C*G*C 5'

Wild Type eGFP gene sequence:

5' TCTGCACCACCGGCAAGCTGCCCGTGCCCTGGCCCACCCTCGTGACCACCCTGACCTA**C**GGCGTGCAGTGCTTCAGCCGCTACCCCGACCACATGAAGCAGCACGACTTCTT '3 NT
3' AGACGTGGTGGCCGTTCGACGGGCACGGGACCGGGTGGGAGCACTGGTGGGACTGGAT**G**CCGCACGTCACGAAGTCGGCGATGGGGCTGGTGTACTTCGTCGTGCTGAAGAA '5 T
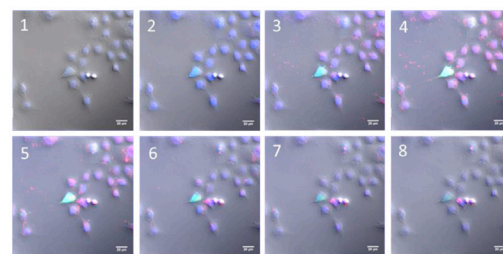
CRISPR	Protospacer (5'-3')
2C	AGCACTGCACGCCCTAGGTC

RNP Components

B

C

D

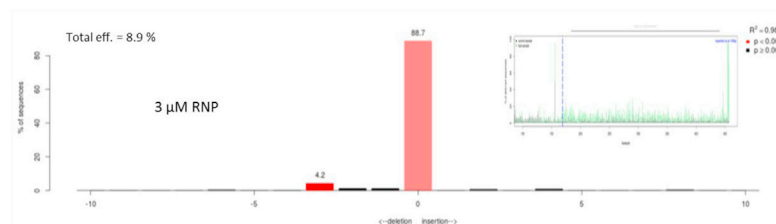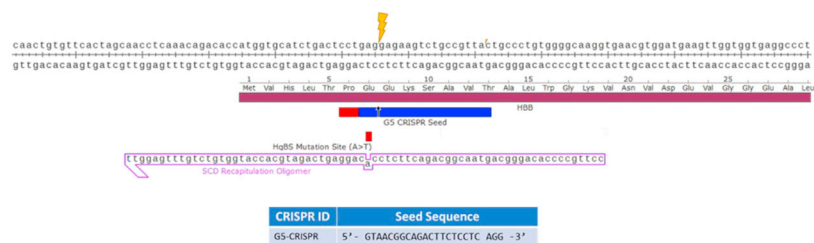| CRISPR ID	Seed Sequence
G5-CRISPR	5' - GTAACGGCAGACTTCTCCTC AGG - 3'

Figure 1. Model System for Gene Editing of the Mutant EGFP Gene

(A) Appropriate segments of the wild-type and mutated EGFP gene with the targeted codon, located in the center of the sequence, are displayed in green and red. The nucleotide targeted for exchange is bolded and underlined. The highlighted bases in blue represent the 2C CRISPR protospacer sequence, and the orange bases highlight

(legend continued on next page)

often does not provide experimental evidence of uptake efficiency that would enable other workers to reproduce or improve upon the effective protocol.

Considering the enormous potential of CRISPR-directed gene editing for inherited diseases in general, and SCD in particular, we have begun a quantitative, systematic analysis of the transfection efficiency of CRISPR/Cas9 and ssODN into CD34+ cells.[8,9] In parallel, we attempt to couple these data to the outcome of gene editing activity at the β-globin locus. We have taken a decidedly reductionist approach, centering our efforts on two types of transfection procedures designed to deliver the CRISPR/Cas9 payload into CD34+ cells: Neon transformation and nucleofection. The overall objective of our work is to use purely physical delivery to introduce both ssODNs and CRISPR/Cas9 RNP into CD34+ cells. We evaluate the relationship between transfection efficiency and gene editing activity based less on conjecture and more on experimental and visual data. To this end, we first analyzed delivery efficiency of RNPs into the cells, followed by an analysis of the viability and status of CD34+ cells during the experimental time frame. We were able to establish robust and reproducible delivery of the RNPs into CD34+ cells. However, we were unable to detect any genomic alteration, including the formation of insertions or deletions (indels), a standard outcome of CRISPR/Cas9 activity using either form of transfection methodology, regardless of whether the vehicle was transported into the nucleus. Our data suggest that more stringent methodological and quantitative optimization of transfection conditions should be undertaken to establish wide-ranging capabilities of introducing genetic change at the β-globin locus.

RESULTS

Efficient Delivery of RNP Particles into HCT116 Cells and Accompanying Gene Editing Activity

Our laboratory has been using HCT116 cells to study the mechanism and regulation of targeted gene editing in mammalian cells.[10–17] As part of this investigation, we have been particularly interested in the relationship between efficient delivery of gene editing tools into the cell and into the nucleus, because it correlates with gene editing activity. We established a test system in which a single copy of the mutated EGFP gene was integrated into HCT116 cells and expanded clonally to create the uniform cell line HCT116-19.[15] The mutation is a single base change in a tyrosine codon, converting a TAC codon to a TAG stop codon, which upon reversion will enable the production of wild-type EGFP and subsequent visualization of a green fluorescence in cells bearing the corrected gene.[18] This reaction has been shown to be catalyzed by ssODNs of a length ranging from 45 to 180 bases in a process known as single-agent gene editing. Using this strategy, we previously determined that approximately 0.5% to 1% of the targeted cell population exhibit the converted phenotype. Addition of programmable nucleases, such as transcription activator-like effector nucleases (TALENs) and CRISPR/Cas9 to the reaction mixture, leads to a substantial increase in correction frequency. In particular, combinatorial targeting with ssODNs and a properly designed CRISPR/Cas9 RNP produces correction frequencies between 6% and 12% routinely. At times, we have seen this frequency elevate to almost 15%, and the reaction depends on the cleavage site generated by Cas9 being located within 50 bases upstream or downstream of the point mutation.[19,20] Yet we do not know whether the activity we observe takes place as a function of the efficient RNP uptake into the target cells. As we began to transition into CD34+ cells, we felt it prudent to investigate and evaluate this potential relationship in a validated and well-established model system that has been used by many laboratories to understand the process of gene editing.

Figure 1A displays the standard targeting model system, with the G residue at the third position of the TAG stop codon highlighted in red; the 180-mer ssODN is also presented. For this particular experiment, we analyzed the transformation of the RNP into HCT116-19 cells using a trans-activating RNA (tracrRNA) labeled with ATTO647 at the 5′ end, which is detected with a 633-nm laser. As part of the assembled and active RNP, we measured the uptake of the RNP into the cells after 24 hr using various dosages, ranging from 0.1 to 0.75 μM. As seen in Figure 1B, when the RNP is introduced into HCT116-19 cells, a sigmoidal pattern of uptake is observed, with a rather large increase seen between 0.2 and 0.5 μM, respectively. The RNP was delivered with a 180-mer ssODN to direct point mutation repair of the mutated EGFP gene, and we coordinately measured the frequency of gene editing activity by analyzing the restoration

the protospacer adjacent motif (PAM) site. The oligonucleotide used in these experiments is 180 bases in length, bearing phosphorothioate-modified linkages at the three terminal bases; the 180-mer targets the non-transcribed (NT) strand (180NT). In the CRISPR/Cas9 ribonucleoprotein assembly reaction, crRNA provides target specificity (20 bases, red section), corresponding to the 2C protospacer sequence, and an interaction domain (blue) with the tracrRNA (green), which has an ATTO647 fluorescent dye attached to the 5′ end. crRNA and tracrRNA are annealed in equimolar concentrations. Cas9 protein (gray) is added to complete RNP assembly. Guide RNAs (gRNAs) direct and activate the Cas9 endonuclease, which then cleaves the target DNA. The lower section of the figure shows the 2C seed sequence and the tracrRNA sequence. (B) Synchronized and released HCT116-19 cells were electroporated with 0.1–0.75 μM at equimolar amounts of CRISPR/Cas9 RNP and 180NT. The tracrRNA used for these experiments has ATTO647 fluorescent dye attached to the 5′ end, which permitted the measurement of RNP transfection. After a 72-hr recovery period, transfection was measured using a FACSAria II flow cytometer. Quadrant 3 shows the cells that were not transfected. Quadrant 4 shows the cells that were positive for CRISPR/Cas9 RNP (ATTO647 fluorescent dye positive). (C) Representative z stack images of HCT116-19 cells transfected with ATTO550-labeled RNP complex 16 hr post-transfection. The z stack top view images show a group of cells with gradual increment of the confocal slices. The green cell in the field of view exhibited gene editing due to a corrected EGFP gene. Blue represents DAPI-stained nuclei, and red represents ATTO550-labeled RNP. (D) Top panel shows the sequence for the HBB gene and the G5 CRISPR seed sequences used in these studies. The oligonucleotide used in these experiments is 72 bases in length, bearing phosphorothioate-modified linkages at the three terminal bases. The 72-mer is used to create a mismatch to produce the sickle cell sequence. Unsynchronized HCT116-19 cells were electroporated with 3 μM RNP with HBB ALT-R G5 CRISPR and 72-mer oligonucleotides (Oligos), both at equimolar amounts. After a 72-hr recovery period, cells were collected. DNA was then isolated, and the HBB gene was amplified and subjected to Sanger sequencing and TIDE analyses to investigate the gene editing activity around the target site.
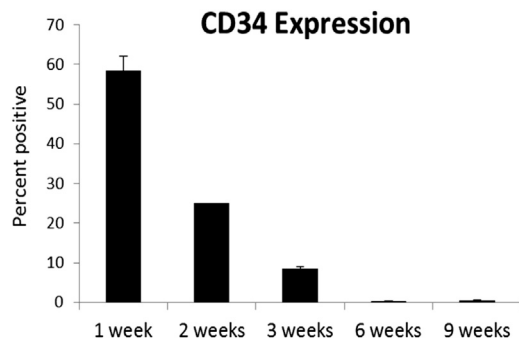
Figure 2. CD34 Surface Marker Expression over a 9-Week Period
PE-labeled anti-CD34 antibody was used to target the CD34+-cultured cells from day 7 through day 63 after the initial cell culture was set up. Cells were analyzed using the BD FACSAria II flow cytometer. The error bars represent SEM.

of productive and visible EGFP production. As can be seen in this figure, while extensive levels of transformation are achieved with as little as 0.1 μM RNP particle using a standard electroporation protocol, significant levels of correction do not appear until 0.5 μM RNP is transfected into the cells. In addition, the data demonstrate that an increase in the dosage of the RNP particle increases the degree of intensity of the labeled molecule in the cells. Altogether, these data suggest that gene editing activity is facilitated when a significant number of RNP particles have entered an individual cell and that high levels of transfection frequency in the absence of highly intense individual cells bearing the RNP is not a sufficient or predictable measure of the outcome of a gene editing reaction.

Figure 1C shows that the transfection results of non-primary cells, HCT116-19 colon cancer cells that harbor the mutated EGFP gene, targeted using CRISPR/Cas9 RNP and ssODNs. The progression of the cell depth is revealed as the slice number of the z stacking increases. RNPs were distributed throughout the HCT116-19 cells, including the nucleus, with noticeable gene correction of EGFP visible in one of the cells in the view. The EGFP-corrected cell exhibits green, while the labeled RNPs are distributed throughout the DAPI-stained nucleus, appearing pinkish as the slice number increases and then disappearing again as the sections reach the cell bottom.

This model system is valuable because it allows us to test the activity of CRISPR/Cas9 RNP particles designed to work at loci unrelated to EGFP. In particular, we can use the HCT116 cells with a validated delivery system to measure the activity of a β-globin CRISPR/Cas9 RNP designed for use in CD34+ cells. Figure 1D shows the sequence of the HBB gene and the G5 CRISPR seed sequence[7] designed to cut at the designated site; the 72-mer ssODN, to direct single base exchange, is also depicted. The RNPs were electroporated into HCT116-19 cells, along with the ssODN at equimolar concentrations. After 72 hr, DNA was extracted from the target cells, the genomic DNA was amplified at the appropriate locus, and the sample was subjected to Sanger sequencing. The results were analyzed using a program known

as Tracking of Indels by Decomposition (TIDE)[21] and are displayed in the lower panel of Figure 1D. These results support the notion that the RNP particle is designed properly so as to be active at the human β-globin locus and is suitable for use in CD34+ cells. In addition, we have previously shown robust gene editing activity at the HBB locus in K562 cells, using the G5-targeting CRISPR/Cas9.[22] When RNPs were developed to target a separate site in the erythroblast Hel92.7 cell line, indel formation was recorded at 77% of the clonal populations that were isolated (data not shown). However, this indel pattern was heavily weighted toward heterozygous knockouts, with only 14% of the analyzed clones exhibiting indel formation in all copies of the gene.

CD34+ Marker Stability in Cultured Cells

The progenitor cells used in this study are characterized primarily by CD34+ surface marker expression and are isolated from primary bone marrow samples. We wanted to determine the length of time that these populations of CD34+ cells maintain some degree of progenitor status after being placed in culture. CD34+ marker expression is highest during the first week of the initiation of cell culture and decreases over time (Figure 2). By day 7, we observe that more than 50% of the cells retain their progenitor characteristics. These data provide some guidance for the establishment of a legitimate experimental workflow and time frame for the optimal addition of gene editing tools.

Optimization of the RNP and ssODN Delivery into CD34+ Cells

After we had verified the activities of all components in the gene editing toolbox, we turned to an examination of the relationship between cellular uptake and reagent delivery to the gene editing activity at the β-globin locus. The targeting system using a CRISPR/Cas9 nuclease and an ssODN, to direct single base exchange, is displayed in Figure 3A. Two Cas9 CRISPR RNA (crRNA) seed sequences, one positioning the cutting activity 1 base downstream of the targeted nucleotide and a second sequence directing cleavage 17 bases downstream of the nucleotide, are illustrated and aligned with the ssODN. The specific break sites on the target gene are indicated by the yellow arrows, and these two seed sequences are designated G5 and G10,[7] respectively. CRISPR/Cas9 is introduced into the cells in the form of a RNP complex. CD34+ cells were transfected with various RNP doses (0.1, 0.2, and 0.5 μM), and uptake was measured via fluorescence-activated cell sorting (FACS) 48 hr later by following the labeled (ATTO550) tracrRNA. Results show a steadily increasing transfection efficiency correlating with increasing levels of intracellular RNP (Figures 3B and 3C).

Although transformation of CRISPR/Cas9 RNPs into progenitor cells has some value for geneticists interested in gene disruption, the conditions for RNP uptake must be evaluated and optimized in the presence of ssODNs, because these molecules are an integral part of reactions designed to repair a point mutation. Because the conditions for transfection established in Figures 3B and 3C led to productive levels of RNP particles in CD34+ cells, we used the same conditions and compared CD34+ cells transfected with RNP alone to cells transfected
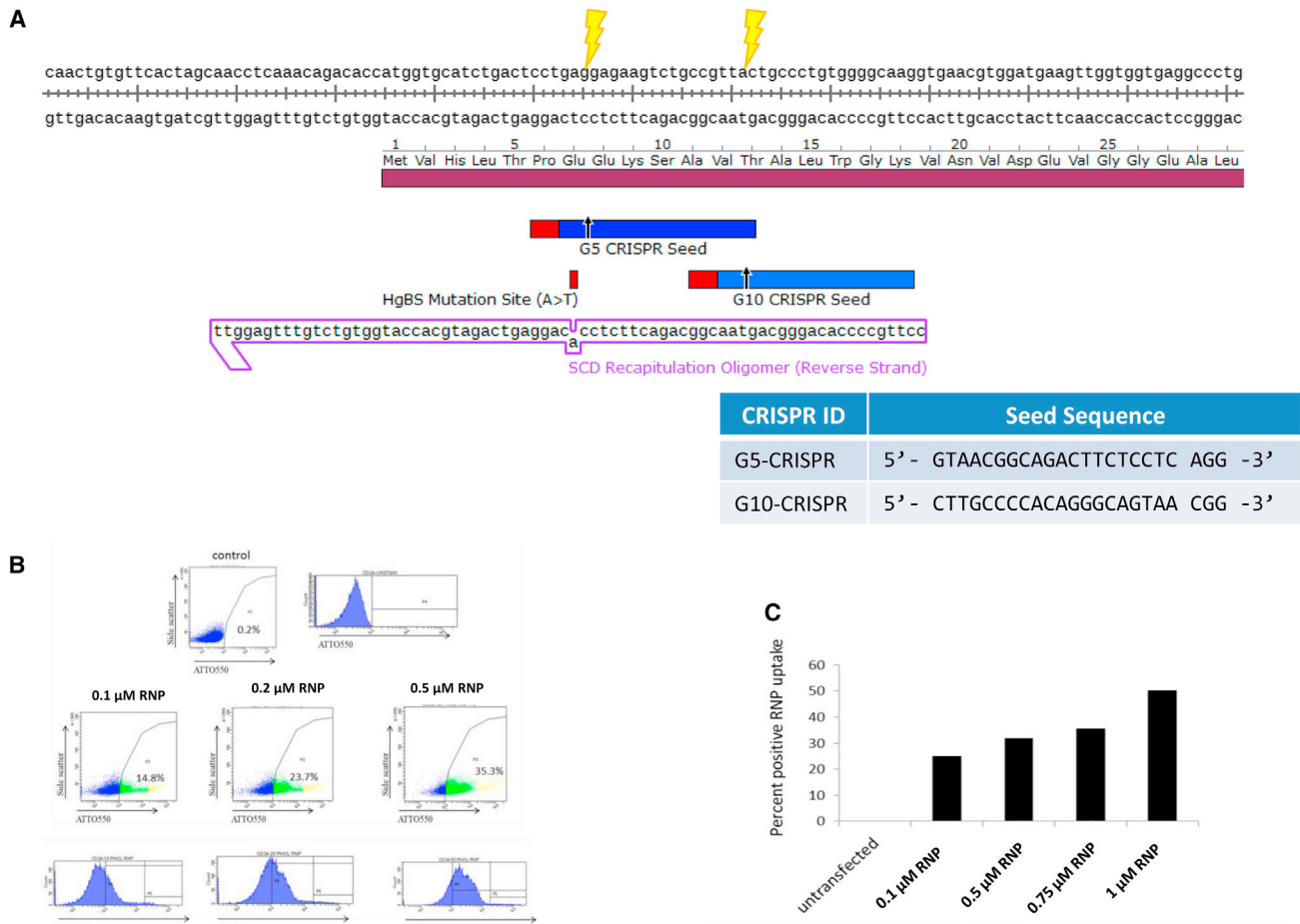
Figure 3. Transfection of CD34+ Cells with Increasing Levels RNP Using a Standard Neon Transfection Protocol

CD34+ cells transfected with different concentrations of RNP and analyzed on the LSR flow cytometer 48 hr post-transfection. (A) Sequences for the HBB gene and the G5 CRISPR and G10 CRISPR seed sequences were used in these studies. (B) Representative dot plots and histograms for cells transfected with increased concentrations of RNP. Gates on the dot plots are set according to the untransfected cells set to 0.2% positive, and the percent positive cells are of the total cell population. (C) Graph represents the percent uptake of the total cells transfected with 0.2 to 1 μM RNP.

with RNP plus the specific 72-mer ssODN (HBB). We transfected CD34+ cells with 0.2 μM RNP, used as our standard RNP concentration, but with two concentrations of the specific ssODN and a non-specific ssODN used previously to target a mutant EGFP gene in HCT116-19 cells. Overall, the results showed the same trend seen in previous experiments: the addition of ssODN at two levels decreased labeled RNP uptake (Figure 4).

The results reported in Figure 4 indicated that the addition of ssODN affects the transfection efficiency of the labeled RNP particle. The next step was to validate the uptake efficiency of ssODN in the CD34+ cells. We reverse the reaction conditions so that the ssODN is labeled instead of the RNP particle. CD34+ cells were then analyzed for successful transformation of a Cy5.5-labeled ssODN, at two levels, using conditions based on information provided by the manufacturer (Integrated DNA Technologies, Coralville, IA). The results are presented in Table S1. The transfection of the ssODN held constant under most of the conditions, with only a modest increase in ssODN uptake observed when the level of the ssODN was doubled. These data suggest that ssODNs are efficiently transfected into CD34+ cells under conditions that also provide detectable and robust levels of RNP uptake.

A significant reaction parameter that is often overlooked in experimental protocols aimed at understanding the transformation of primary cells is the time at which uptake is analyzed. Once we had confirmed coordinated RNP and ssODN uptake from 24 to 48 hr, we carried out an experiment in which the same conditions used in the data presented in Table S1 were tested by varying the time at which the experiment was ended. The results of these experiments are presented in Figure 5A and reveal significant RNP uptake at early times during the reaction period, coupled to a decrease in RNP uptake as reaction time is increased from 16 to 72 hr. These results represent the optimized conditions, and because a significant amount of
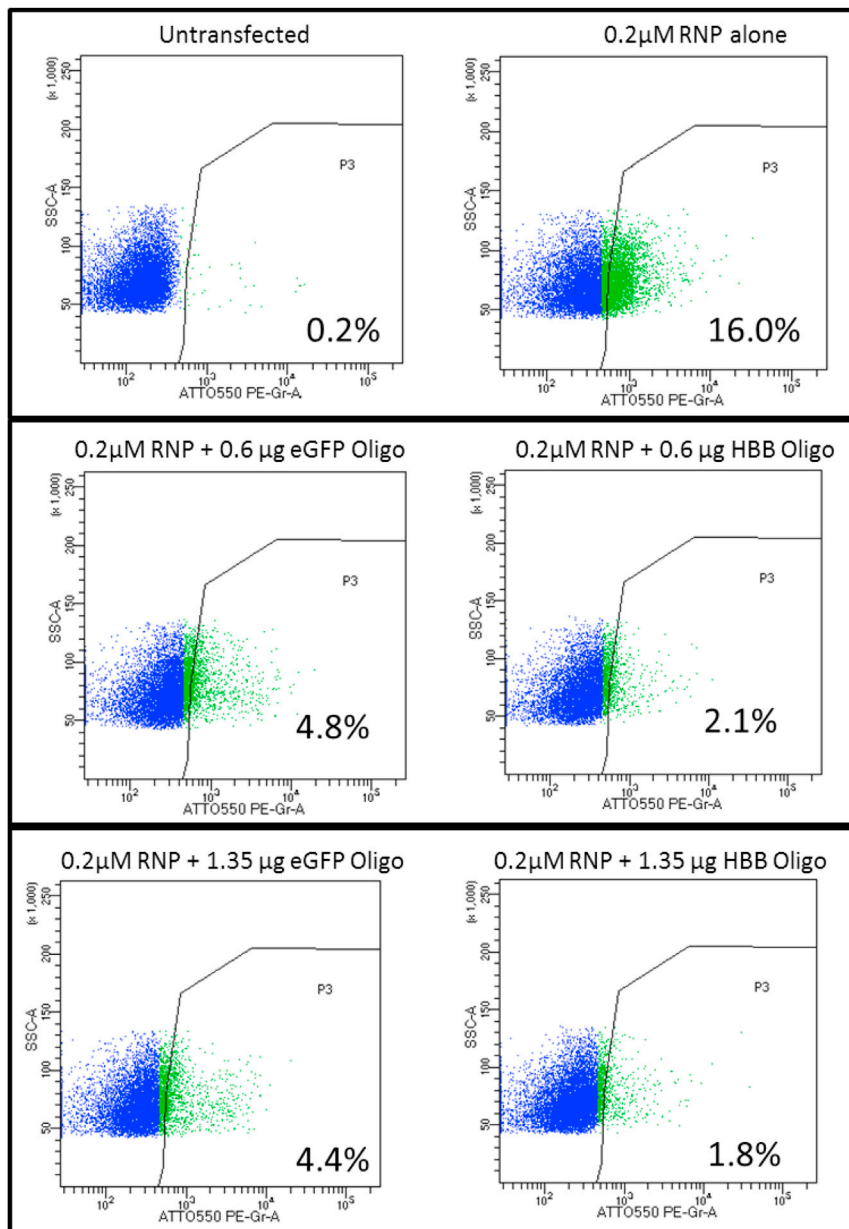
Figure 4. Transfected CD34+ Cells Analyzed 24 hr Post-transfection with the Addition of ssODNs

CD34+ cells were transfected with 0.2 μM RNP and analyzed 24 hr post-transfection for percent RNP uptake. The results show the addition of HBB 72-mer Oligo and EGFP Oligo both decrease the RNP uptake, but to different degrees. The concentration of the oligo did not seem to change the percent uptake. The dot plots show representative flow cytometry graphs from one set of transfections, and the table shows the range of numbers observed in the experiments. All transfections were performed using the standard Neon transfection protocol.

CD34 cell transfections	average percent uptake
untransfected	0.0
0.2μM RNP alone	22.3% $\pm$ 9.0
0.2μM RNP + 0.6μg HBB Oligo	2.1% $\pm$ 0
0.2μM RNP + 1.35μg HBB Oligo	1.9% $\pm$ 0.1
0.2μM RNP + 0.6μg GFP Oligo	4.9% $\pm$ 0.1
0.2μM RNP + 1.35μg GFP Oligo	4.5% $\pm$ 0.1

A

CD34 cells transfected with 0.2 μM RNP

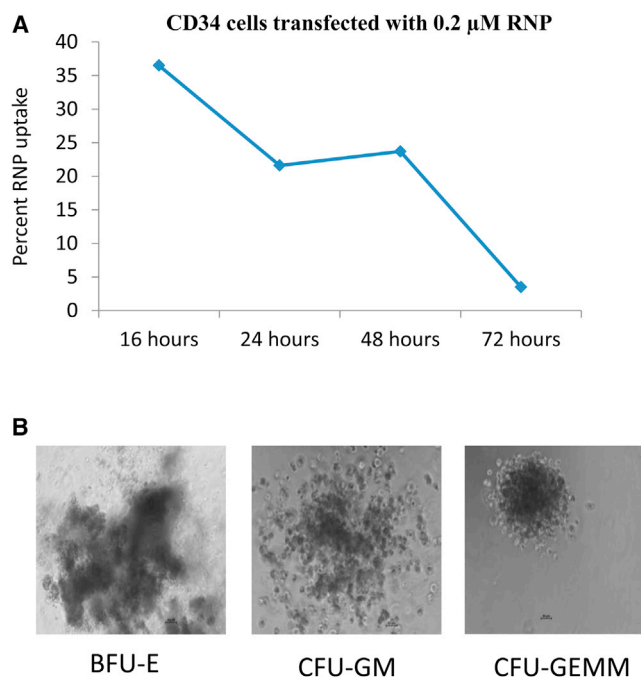
B

BFU-E CFU-GM CFU-GEMM

Figure 5. Analysis of CD34+-Transfected Cells with RNP

(A) Cells were transfected with 0.2 μM RNP alone and analyzed at the designated time points post-transfection. Percent uptake represents the positive cells out of the total cell population. These transfections were performed using the Neon system. (B) Representative images of CD34+ single-cell-derived colony types. After transfection, CD34+ cells were sorted and grown in plates with MethoCult medium, over a 14-day culture time, and images were taken of the colonies under a 10× objective using a bright-field microscope.

transfection occurred, we proceeded to carry out single- and multiple-cell cloning of CD34+ cells.

Both single- and multi-cell sorts were performed and plated in MethoCult to obtain clones (see Methods and Materials). Cells were sorted as described in Methods and Materials and allowed to grow for 14–16 days in culture. CD34+ cells differentiated into four main types of colonies from both single-cell sorts in the 96-well plate and mixed single-cell culture in the 6-well plates. Representative images were taken, and the colony types were characterized based on the phenotypic differences (Figure 5B). The colonies obtained from the targeting experiment showed the differentiation of the CD34+ cells into colony-forming unit-erythroid (CFU-E); burst-forming unit-erythroid (BFU-E); colony-forming unit-granulocyte, macrophage (CFU-GM); and colony-forming unit-granulocyte, erythroid, macrophage, megakaryocyte (CFU-GEMM) colonies.

Genetic Analyses of Gene Editing Activity

The data demonstrating efficient cellular uptake using the combination of the RNP and ssODN prompted us to analyze the outcome of gene editing at the β-globin locus. As shown previously in Figure 3A, two seed sequences create a double-stranded break 1 or 17 bases downstream of the target nucleotide. The ssODN designed to

direct nucleotide exchange is also depicted below the G5 and G10 seed sequences. We used our optimal transfection conditions, as defined earlier, and targeted the β-globin gene for single base change through the action of the RNP and the ssODN. Then, 24 hr after introduction of the RNP particle into the CD34+ cells, genomic DNA was isolated and sequenced by Sanger sequencing. Sequences were analyzed to identify any gene editing activity within the whole-cell population through the use of TIDE (described earlier). This program analyzes DNA based on multiple stretches of sequence alignment. First, the program determines where the CRISPR/Cas9 cleavage site is located by comparing the imported seed sequence to the sequence of the wild-type control sample chromatogram. Once this cleavage site is determined, TIDE generates an alignment window, stretching from a supplied base number (default, 100 bp) to 5 bp upstream of the CRISPR cleavage site. This window is then used to align the control sample chromatogram with the test sample chromatogram, the sequence file of the CRISPR/Cas9-treated samples. Once alignment of the test and control chromatograms is achieved, TIDE is ready to determine indel size. A decomposition window is generated, with the left and right boundaries being determined by the user along simple guidelines: the left boundary must be located x bp from the cleavage site, where x is the indel size range + 5 bp. As seen in the upper panel of Figure 6A, we were unable to detect any indel formation or single base change within the population of CD34+ cells in a reaction containing either the G5 or the G10 crRNA seed sequences. We also performed numerous experiments with unlabeled RNP and locked nucleic acid (LNA)-modified RNPs (Figures S3A and S3B) and still did not see robust indel formation. We wanted to rule out any effect of the label on the RNP and interference with genetic activity.

We next carried out the same analyses on populations of cells that had been grown as a single clone. The clonal expansion was generated by placing a single CD34+ cell isolated from the population of targeted cells into a 96-well plate, as described earlier. As seen in the lower panel of Figure 6A, we again find no evidence of indel formation or see evidence of the single base change in the 28 clones analyzed. Small bars at other indel size positions of the TIDE-produced graph (in black) are artifacts generated by the low level of background present in the analyzed sequence file; a p value of 0.001, as determined by the readable length of an individual subsequence, is required to be considered a significant indel.

Finally, we pushed the limits of using RNP concentrations well above any reported concentrations to see whether we could push indel formation while maintaining some cell health. To this end, we performed experiments using 3 μM (300 pmol) RNP, with and without modifications, as seen in Figures S3A and S3B, but also 5 μM (500 pmol) RNP with non-significant indel formation (data not shown).

Visualization of RNP Uptake into CD34+ Nuclei and Associated Gene Editing Activity

The lack of genetic modification directed by the RNP and ssODN was puzzling, particularly with previously published methods and results

A

B

C
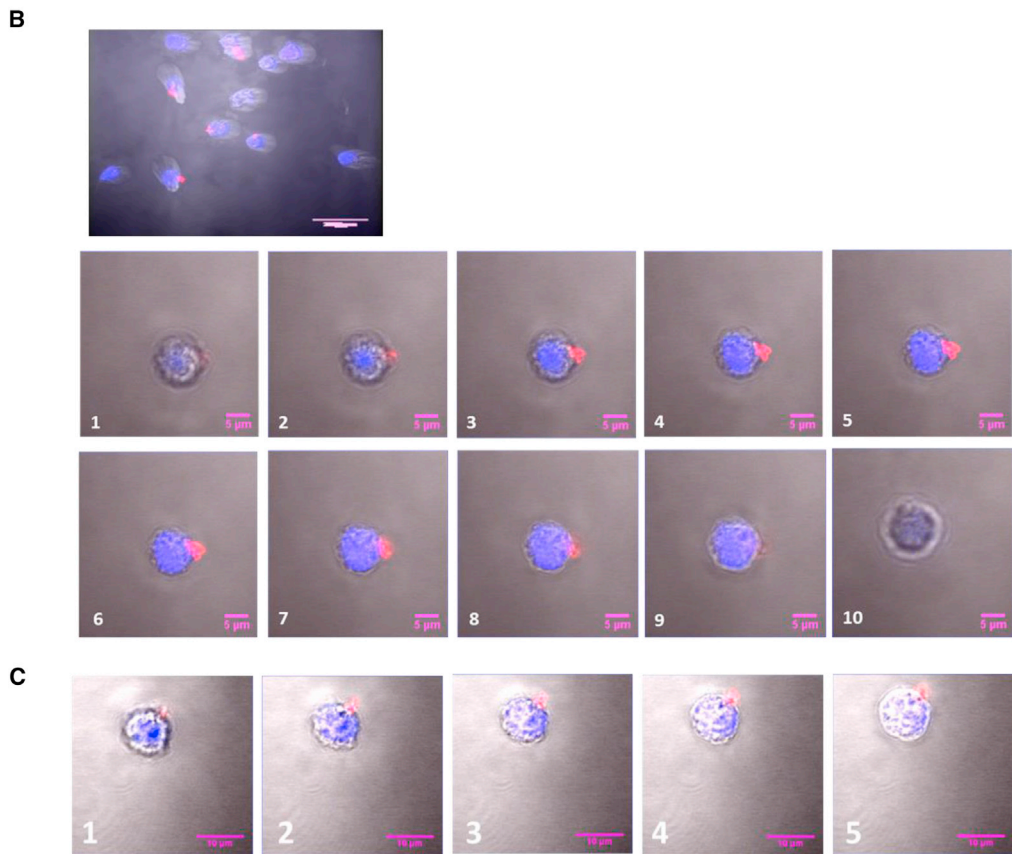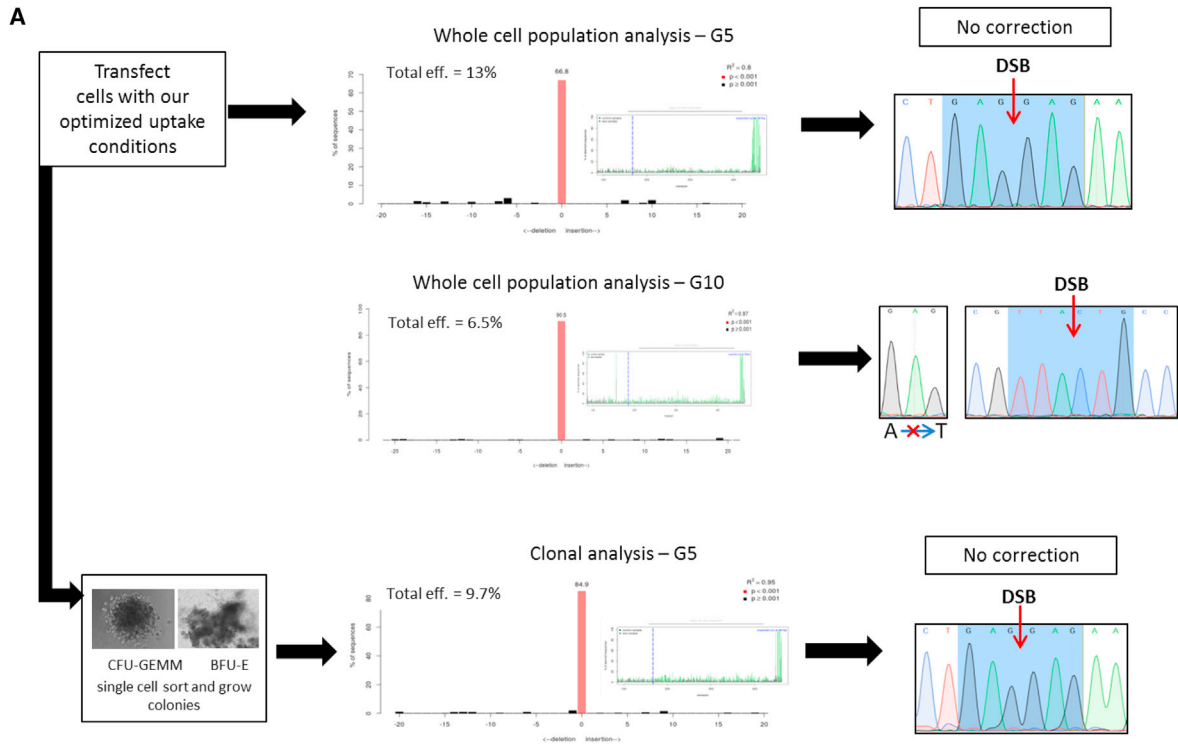
(legend on next page)

that indicated otherwise. We reasoned that the RNP and the ssODN may be efficiently introduced into the body of the cell but may not be penetrating the nuclear membrane with sufficient efficiency to enable genome modification. Thus, the CD34+ cells were transfected with the ATTO550-labeled RNP using our standard Neon transformation protocol, as described in Methods and Materials. The ATTO550-labeled RNP (with labeled tracrRNA) appeared red, and the DAPI-stained nuclei appeared blue. The RNP tends to form clusters, and as shown in Figure 6B, the RNP reached only the outside of the nuclear membrane; it was not dispersed within. In addition, we tested an ATTO550-labeled crRNA in Figure 6C to make the RNP complex and again saw similar results of RNP clusters outside of the nuclear membrane. These results support the notion that the RNP did not enter the nucleus at a level that enabled gene editing activity, and the results are similar when either RNA molecule harbors the ATTO550 label in the RNP complex.

The apparent disconnection between transfection efficiency and gene editing activity prompted us to use a different type of genetic transfer system. One of the most popular is nucleofection, primarily applied through a Lonza transfection system. For these experiments, we employed conditions suggested by the manufacturer that presumably had been optimized for the delivery of gene editing tools into CD34+ cells. We carried out the same type of experiment and analysis that had been previously described for uptake of the labeled RNP and ssODN depicted in Figure 3. The amount of labeled RNP was measured after 16, 24, 48, or 72 hr, and the results are depicted in Figure 7A. In comparison to the cellular uptake promoted by the Neon electroporation system, nucleofection appears to deliver a higher percentage of labeled RNP into the cells at each time point. Similar to the results produced from Neon transformation, however, the amount of RNP remaining in the cell appears to diminish as a function of time. Figures 7B and 7C exhibit the results of confocal microscopy using z stack analysis, demonstrating that in most cells (a specific example is depicted herein), the labeled RNP particle appears to have traversed into the nucleus, as evidenced by the blending of blue and red to generate a pink opaque color within the nucleus. This result stands in contrast to the results obtained with Neon transformation measured similarly by z stack analysis (Figures 6B and 6C).

Because a larger percentage of the CD34+ cells was found to contain the labeled RNP, and confocal microscopy revealed a high degree of

nuclear delivery, we undertook genetic analysis of the transfected population via indel formation and TIDE analyses. The experimental protocol was identical to the protocol used to generate the data presented in Figure 6. We again detect no significant indel formation and no point mutation change directed by the co-transfected ssODN (HBB) (Figure 7D). To maximize the possibilities of detecting indel formation, the results depicted in the two panels of Figure 7D were generated using 3 μM G5 or the G10 seed sequence.[7]

DISCUSSION

The acclaimed genetic engineering tool, CRISPR/Cas9, will realize its full potential when robust and reproducible methods for delivering the package into primary cells are fully developed. It is widely accepted that improving the transport efficiency into the cell, and moreover into the nucleus, is the benchmark of success for generating a genetically altered genome. The data reported in this paper suggest otherwise. A short literature review produces an overwhelming number of strategies for delivering gene editing tools into primary cells, none of which appear to have significantly overlapping or complementary steps. For example, although it seems that gene editing in CD34+ cells using the RNP appears to be straightforward and well established, numerous discrepancies exist, thereby confounding and limiting the robustness of this approach. Two common methodologies, Neon transformation and nucleofection, are employed by a variety of laboratories, but within each group, different instrument settings, different concentrations of CRISPR/Cas9, and different sources of CD34+ cells are used (Table 1). In addition, the methodology of preparing the CD34+ cells for transformation varies widely, and descriptions outlining these treatments are often vague, making attempts at reproducing the work challenging at best (Table 1).

In this work, we begin the reinvestigation (and perhaps reestablishment) of suitable and valid benchmarks that might be foundational and robust for a translatable and applicable gene editing system for SCD. We have taken a decidedly reductionist approach by examining the fundamental relationship between delivery and detectable gene editing activity. We chose to use bone marrow-derived cells for our analyses because this source of primary cells is the most practical and logical for clinical implementation of this technique in patients. The use of patient-derived bone marrow cells would provide the best option for impactful gene editing, with the caveat of patient health concerns that could arise during the process.

Figure 6. Transfection of CD34+ Cells Using the Two RNP Complexes with 1 μg of ssODN

(A) Cells were transfected with RNP, using the optimized Neon transfection parameters, and sorted 24 hr post-transfection based on ATTO647-labeled cells. A portion of the transfected cells was collected 24 hr post-transfection and analyzed as whole-cell populations. No correction was seen in the whole-cell population at either the G5 or the G10 site, but the G5 site gave more indel formation, so single-cell clonal analysis was performed. Single cells were sorted into each well of a 96-well dish that was pre-coated with MethoCult. After 20 days in culture, colony types were obtained and collected for clonal analysis. No correction was seen at the target site in any of the clones. In total, 28 clones were analyzed. The cells analyzed from this experiment were transfected with the Neon system. (B) Representative z stack images of CD34+ cells transfected with ATTO550-labeled tracrRNA to make the RNP complex, 16 hr post-transfection. The top panel shows cells that were transfected using the Neon system with optimized uptake conditions. This is a representative image showing a field of cells, top view (left) and side view (right), with a lack of nuclear RNP localization. The bottom series of images represents a single CD34+ cell post-transfection. The images are shown in numerical order from 1 to 10, representing images from the top of the cell to the bottom. The images show a lack of true nuclear localization of the RNP complex in the cell. The RNP complex appears to be blocked near the outside of the nuclear membrane. (C) Representative z stack images of CD34+ cells transfected with ATTO550-labeled crRNA to make the RNP complex, 16 hr post-transfection.
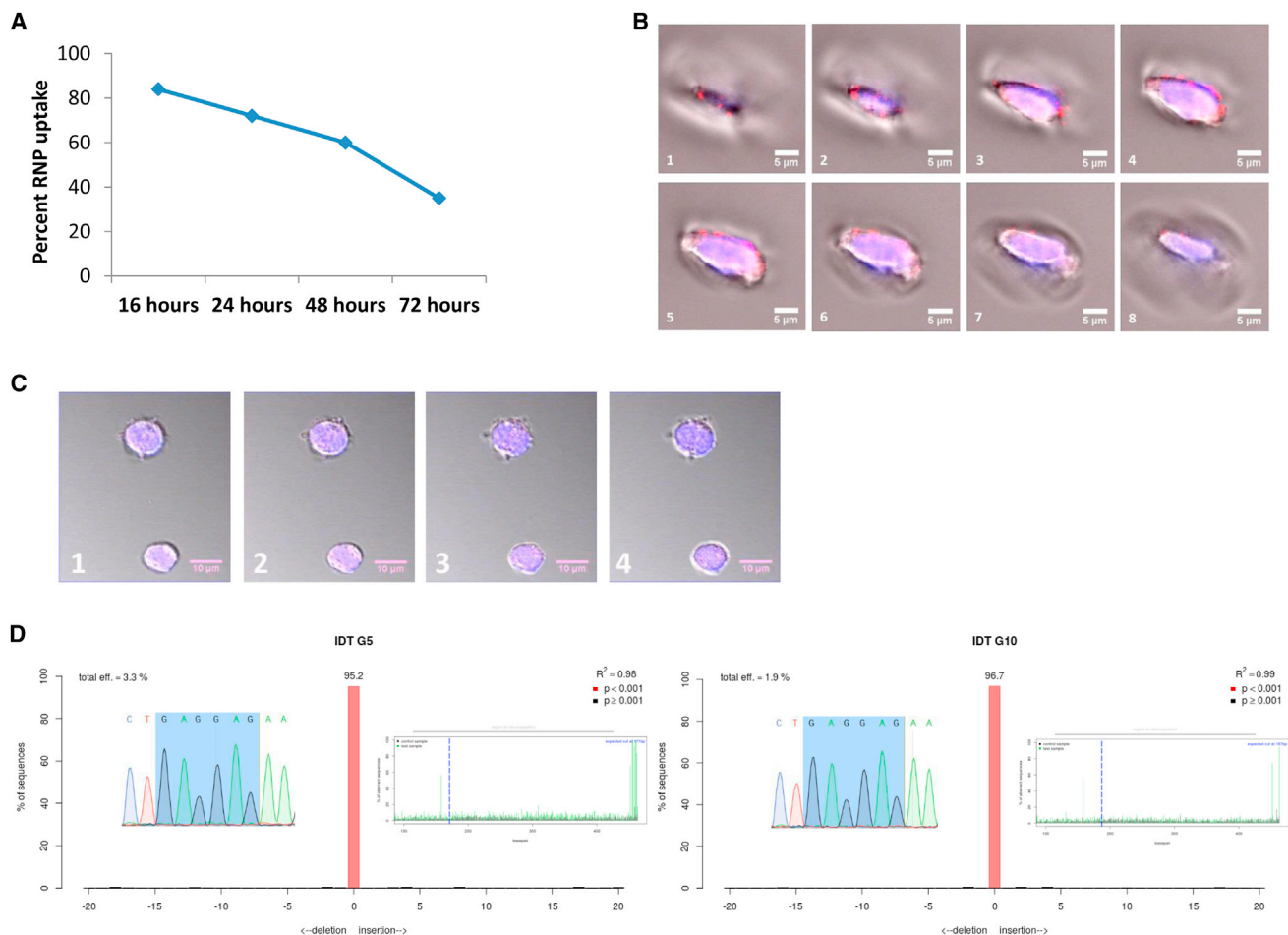
Figure 7. Cellular and Genetic Analysis of the Population of CD34+ Cells Transfected with Labeled RNP Using Nucleofection

(A) Cells were transfected with 0.2 µM RNP and analyzed at the designated time points post-transfection. Percent uptake represents the positive cells out of the total cell population. These transfections were performed using the Nucleofector 2B device. The images show clear nuclear localization of the RNP complex. There is also some RNP complex that appears to be blocked near the outside of the nuclear membrane. (B) Representative z stack images of CD34+ cells transfected with ATTO550-labeled tracrRNA to make the RNP complex 16 hr post-transfection. The images are shown in numerical order from 1 to 8, which represent images from the top of the cell to the bottom. (C) Representative z stack images of CD34+ cells transfected with ATTO550-labeled crRNA to make the RNP complex, 16 hr post-transfection. (D) Cells were transfected and collected 72 hr post-transfection for whole-population TIDE analysis.

To establish a baseline relationship between delivery and successful gene editing, we first used a well-established gene editing system in which all reaction components have been validated and clearly defined.[18] We report that although significant RNP delivery is achieved at low concentrations, a significant level of gene editing activity is realized only when the highest levels of RNP are electroporated into the cell. We also show that nuclear delivery is easily achieved in the HCT116-19 cell model systems. These observations lead to the hypothesis that there is no direct correlation between efficient cellular uptake and genome modification directed by an RNP.

We translated the reaction parameters that enabled activity in HCT116-19 cells to bone marrow-derived CD34+ cells, replacing the mutant EGFP gene with the human β-globin gene. We found that CD34+ cells maintain phenotype for approximately 1–2 weeks, suggesting that experiments must be carried out during this time frame to achieve targeting of CD34+ cells within this dynamic and evolving population. Dose-dependent uptake conditions of both RNP and specifically designed ssODNs that were optimized for Neon transformation and nucleofection were obtained. Uptake into target cells was also time dependent, because measurements of delivery efficiency were altered as a function of the time at which uptake is analyzed. This analytical parameter is important, because primary publications reporting successful gene editing in CD34+ cells routinely report that the best time to analyze uptake lies between 24 and 48 hr. Our targeted population is capable of developing into a variety of colonies grown and MethoCult media over a 14-day time frame, including colonies that exhibit BFU-E, CFU-GM, and CFU-GEMM phenotypes. Because these colonies appear readily in culture, the mechanism of delivery does not depress cell viability or cell destiny.

Table 1. Delivery Options for CD34+ Gene Editing

CD34+ Cell Source	Culture Conditions	No. Cells Transfected	Kit for Transfection	Mode of Transfection	CRISPR/Cas9	Reference No.
Mobilized peripheral blood	NA (X-VIV015 media + cytokine supplements)	500,000	P3 Primary Cell 4D-Nucleofector kit	Lonza 4D-Nucleofector (program EO-100)	10 μg sgRNA, 15 μg Cas9 mRNA. and 1 μg plasmid	28
Mobilized peripheral BM and CB	1–2 days cells in culture before transfection (StemSpan SFEM II media + listed cytokines)	5 million–80 million	Human T Cell Nucleofector kit	Nucleofector 2b device (program U-014)	Cas9 protein/sgRNA or Cas9 mRNA/sgRNA + AAV6 donor vector	2
Mobilized peripheral blood	24 hr cultured cells before transfection (StemSpan SFEM + CC110 cocktail)	100,000–200,000	Lorita P3 solution	Lonza 4D-Nucleofector (program 00100 or ER1 OO)	72–200 pmol Cas9 RNP + 100 μM ssDNA	26
Peripheral blood of SC patients	cells expanded 7 days before transfection (StemSpan SFEM II + CC100 cytokine cocktail)	5,000–10,000	Human CD34 Cell Nucleofector kit	Nucleofector 2b device (program U-008)	1st electroporation, l0μg Cas9 mRNA; 2nd electroporation, sgRNA and HDR template	29
Peripheral blood and CB	2 days in culture before transfection (StemSpan + cytokines)	150,000–250,000	Neon Transfection System (10 μL kit)	Neon Transfection System (1,600 V, 10 ms, 3 pulses)	200 ng-1 μg sgRNAs + 1 μg Cas9 protein	6
CB and BM of SCD patients	2 days in culture before transfection (X-VIV015 + cytokines)	200,000	BTXpress buffer	BTX ECM 830 Square Wave Electroporator (250 V, 5 ms)	ZFN mRNA + oligonucleotide	30
Mobilized peripheral blood	NA (not easily found)	1 million–5 million	NA	Nucleofector 2b device (program U-008)	2 × 10 μg DNA plasmid encoding gRNA, Cas9, and GFP	31

The options available for the delivery of gene editing tools into CD34+ cells. BM, bone marrow; CB, cord blood; HDR, homology-directed repair; NA, not applicable; ssDNA, single-stranded DNA; SC, sickle cell; ZFN, zinc-finger nuclease.

As presented in Figures 6 and 7, we find no relationship between cell delivery and gene editing activity. It is possible to explain the negative results generated from cells that have undergone Neon transformation, because z stack confocal microscopy images indicate that the labeled RNP did not enter the nucleus. Rather, the RNP appears to assume a punctate conformation localized at the surface of the nuclear membrane. However, the results are more perplexing when we analyze genetic data from samples in which the RNP was introduced by nucleofection. Here, despite abundant nuclear uptake, no gene editing activity was detected.

Furthermore, we tested two HBB single guide RNAs (sgRNAs) (G5 and G10) as sgRNAs complexed with Cas9 protein. The sgRNAs were generated synthetically and transfected under similar concentrations (1 μM RNP). We noted a minor increase in indel formation. This seems to be the most robust step for gene editing in bone marrow CD34+ cells, and we have found that other labs are having success with gene editing using these synthetically made sgRNAs in both cord blood and mobilized CD34+ cells. In addition, we tested the efficiency of in vitro-transcribed sgRNA and found a similar minor increase in indel formation in bone marrow-derived CD34+ cells.

Many reports touting success of gene editing for SCD and thalassemia in CD34+ cells use cord blood-derived cells instead of bone marrow-derived cells.[23–26] Reasons for the choice of cord blood cells are the differences in telomere dynamics, cell-cycle progression, differential gene expression profiles, and most importantly, autocrine production of cytokines.[25] Cord blood contains more primitive progenitors that are multi-potent and have long-term culture-initiating cells. They possess higher proliferation and expansion potentials and have superior capacity for self-renewal compared to bone marrow- or peripheral blood-derived cells.[25] These cellular metabolic characteristics may be why cord blood-derived cells, while perhaps impracticable for therapeutic use, are more amenable to gene editing activity. Although cord blood-derived cells are superior in many aspects, there are some serious drawbacks. To have successful adult cell transplantation, many CD34+ cells will be required: one unit of cord blood may minimally benefit a child, but several units of cord blood would be necessary to provide benefits to an adult.[23,25,26] A second major hurdle is the significant delay in engraftment seen with cord blood cell transplantation into adults compared to bone marrow or mobilized peripheral blood transplants.[23,24] Finally, cord blood contains a low number of naive T cells, which make the immune recovery after umbilical cord blood transplantation low, leaving the recipients more prone to severe infections.[23]

So why have we been unable to observe genetic conversion in CD34+ cells? A simple reason is that we established strict and conservative parameters to judge both cellular or nuclear uptake and gene correction. Considering the difficulty in transferring experimental protocols

from lab to lab, we feel that a more conservative methodical approach is warranted. Another reason may be that we designed our CD34+ cell experimental protocol based on the levels of RNP required to produce significant point mutation repair and indel formation in HCT116 cells (Figure 1). This was done purposely, because our goal is to set a foundation for the correlation of cellular uptake and gene editing events; the molar ratio of RNP particles to target gene in CD34+ cells still exceeds 100,000. If we were to increase the amount of RNP introduced into cells, as others have done,[27] we would likely be able to force gene editing activity and produce results. But this experimental strategy comes at a price, because the viability of the cell population would be adversely affected and translation into the clinical setting would become highly problematic. In the long run, gene editing of specific mutations must occur with a concurrent maintenance of cell viability. Increasing the amount of genetic tool simply to achieve a specific outcome is not, in our opinion, a scientifically meritorious approach. The data reported in this manuscript may begin to establish the basis for carving out guidelines as to how best to evaluate practicality and efficiency of gene editing activity in CD34+ cells for clinical application, particularly for SCD.

MATERIALS AND METHODS

Cell Culture Conditions

Bone marrow CD34+ cells were purchased from Stem Express (Folsom, CA). Cells were thawed according to the manufacturer's protocol and grown in StemSpan serum-free expansion motif (SFEM) II (STEMCELL Technologies, Vancouver, BC) supplemented with StemSpan CD34+ Expansion Supplement (STEMCELL Technologies, Vancouver, BC). Cells were cultured in suspension, maintained at 0.5×10^6–1.0×10^6 cells/mL, and incubated at 37°C and 5% CO_2. Cell number was evaluated using Countess FL (Life Technologies, Carlsbad, CA), and culture medium was changed when cell viability would drop below 85%. All cells before transfection were ≥90% viable and only in culture for 4–5 days. HCT116-19 cells were cultured as previously described.[18]

CD34+ Progenitor Determination

CD34+ expression over time was analyzed using a phycoerythrin (PE)-conjugated mouse anti-human CD34 antibody (BD Biosciences, catalog No. 50941) and compared to a PE-conjugated mouse anti-human immunoglobulin G (IgG) control (BD Biosciences). 200,000 CD34+ cells were harvested for each time point of analysis. The appropriate antibodies were added to the cell suspensions and incubated at 37°C for 30 min. The cells were washed twice with PBS and analyzed by flow cytometry. Samples were run at the Center for Translational Cancer Research (CTCR) Flow Cytometry Core Facility at the Helen F. Graham Cancer Center & Research Institute (HFGCC&RI), using the BD FACSAria II flow cytometer, or at the Wistar Flow Cytometry Facility (Philadelphia, PA).

Assembly of Cas9 RNP Complex

The recombinant Cas9 protein, ATTO647-labeled tracrRNA, ATTO550-labeled tracrRNA, HBB gene targeting custom-made crRNAs (G5 and G10), ATTO550-labeled crRNA, and EGFP crRNA were a gift from IDT (Integrated DNA Technologies, Coralville, IA). The sequences can be found in Table S2. The individual components were reconstituted to make the RNP complex at various molar ratios of protein and RNA, 1:1 Cas9 to crRNA and tracrRNA. The RNP complex was built and used according to the Alt-R CRISPR/Cas9 System transfection protocol provided on IDT's website.

Optimization of the Delivery of Cas9 RNP Complex and ssODNs

We varied the RNP concentrations from 0.1 to 0.75 μM and ssODNs from 0.6 to 1.35 μg in 2.0×10^5 CD34+ cells, and the Neon Transfection parameters were optimized with voltage (1,150–1,700 V), duration (10–40 ms), and pulse (1–3). The Neon Transfection 100 μL kit with buffer R was used for these experiments. The total volume of cell solution and transfected materials added did not exceed 110 μL. The optimal condition for RNP delivery into the CD34+ cells was found to be 1,600 V, 10 ms, and 3 pulses. The transfected CD34+ cells were transferred into 6-cell plates containing 2 mL of pre-warmed, complete CD34+ cell culture medium. The cells were grown in the culture for 16–72 hr, harvested, and subjected to flow cytometry for delivery efficiency of the ATTO-labeled RNP complex. For optimization experiments on CD34+ cells, a HBB gene targeting custom-designed 72-mer ssODN was synthesized by TriLink.

Clonal Expansion of HBB-Edited CD34+ Cells

Two methods of performing clonal expansion of HBB-edited CD34+ cells were carried out. One method was to mix the bulk amount of cells that have undergone gene editing with MethoCult Express medium and plate in 6-well plates for colony formation. The other procedure was to sort the ATTO-labeled, RNP-containing CD34+ cells as single cells into each well of a 96-well plate for clonal expansion. Each well of the 96-well plate had 100 μL of MethoCult pre-plated before FACS. The single cells were allowed to grow for 14–16 days in culture until colonies were fully developed. The CD34+ cells differentiated into four main types of colonies. The colony types were classified as CFU-E, BFU-E, CFU-GM, or CFU-GEMM. The descriptions of each colony classification can be found in the manufacturer's manual (STEMCELL Technologies). Each colony was taken out of the MethoCult medium by diluting with pre-warmed PBS and collecting the samples in Eppendorf tubes. Each tube was spun down for 10 min at $100 \times g$, and the cell pellets were frozen at −20°C for DNA isolation, HBB gene amplification, and sequencing.

Confocal Microscopy

CD34+ cells were transfected with either ATTO550-labeled tracrRNA- or ATTO550-labeled crRNA-complexed CRISPR/Cas9 RNP using the Neon system or Nucleofector 2B device. Then, 24 hr after the delivery of the CRISPR/Cas9 RNP, CD34+ cells were harvested and spun down at 700 rpm for 5 min. The cells were washed once with PBS and fixed with BD Cytofix/Cytoperm Fixation and Permeabilization Solution at 4°C for 20 min. Cells were rinsed with PBS, centrifuged at 700 rpm for 5 min, resuspended in 15 μL of PBS, and transferred onto a microscope slide. A drop of ProLong Diamond Antifade Mount with DAPI (Life Technologies) was applied onto the cells, and a #1.5 coverslip was placed atop to complete the

preparation of the microscope sample. A Zeiss LSM880 laser scanning confocal microscope at the Delaware Biotechnology Institute (DBI) was used to visualize and acquire the 3D multi-channel data. A 63× oil objective lens and channel light sources (bright-field-transmitted light and 405- and 561-nm lasers) were used. The ATTO550-labeled RNP is shown in red, and DAPI-stained nuclei appear blue. HCT116-19 cells post-electroporation were grown in Nunc Lab-Tek II Chambered Coverglass plates for 72 hr, rinsed with PBS, and fixed with BD Cytofix/Cytoperm Fixation and Permeabilization Solution at 4°C for 20 min. The fixation solution was aspirated, cells were rinsed with PBS twice, and a drop of ProLong Diamond Antifade Mount with DAPI (Life Technologies) was applied on the cells. The treated cell samples were investigated under a Zeiss LSM880 laser scanning confocal microscope at DBI. A 63× oil objective lens and four channel light sources (bright-field-transmitted light and 405-, 488-, and 561-nm lasers) were used. To construct the 3D images of the cells, z stacking and 3D building functions of the confocal microscope system were used. The z stacking slice intervals were set as 280 nm, and the pixel size was selected as 1,024 × 1,024 pixels. An average of 4 or 8 scanning data per light channel were acquired for each sample. The image data were processed to construct stationery images of 3D movies using ImageJ (NIH).

Gene Editing Reactions

The combination of the 72-mer NT ssODNs and Cas9 RNP complex was used to convert the A-T base change of the HBB gene in CD34+ cells. The Neon transfection delivery method, cell number, and conditions were the same as in the RNP uptake experiments except for the addition of various amounts of the 72-mer ssODN. 3 μM RNP complex concentrations were used per gene editing reaction. In addition, for the nucleofection experiments, Nucleofector 2b device was used. 200,000 CD34+ cells were harvested, centrifuged at 100 × g, and suspended in Human CD34+ Cell Nucleofector Solution (Lonza, Basel, Switzerland) to a final concentration of 2.0 × 10^5 cells per 100 μL of buffer. The total volume of cells, RNP complex, and 72-mer ssODN was transferred to the certified Nucleofector 2B device cuvette. The sample was electroporated using Nucleofector 2B device U-008. After electroporation, the cells were resuspended in 500 μL of supplemented culture medium and carefully transferred into 6-cell plates containing 2 mL of pre-warmed, complete CD34+ culture medium. The cells were grown in the culture for 72 hr and harvested, and genomic DNA was isolated for sequencing. The sequencing data were analyzed for sickle cell mutation conversion and damage assessment using the software program TIDE (Netherlands Cancer Institute, https://tide.nki.nl/). HCT116-19 cells were targeted and analyzed as previously described.[18] The Bio-Rad Gene Pulser was used[18] to deliver the RNP and the ssODN. EGFP targeting custom-designed 180-mer oligonucleotide was synthesized by IDT (Integrated DNA Technologies, Coralville, IA).

DNA Sequencing and Mutagenesis Analysis of the CD34+ and HCT116-19 Genomic DNA

PCR products were verified by DNA sequencing by Genewiz (Union, NJ). Individual CD34+ cell clones were analyzed by TIDE to determine individual sub-sequences within the multi-peaked breakdown product after CRISPR/Cas9 activity. The TIDE analyses provide a visual of the sequence decomposition, the indel patterns of the clone, and the relative ratios of each clonal indel pattern, serving as an intermediate step in determining each allelic profile. By using the indel patterns and their relative ratios provided by TIDE, the control trace sequence and a clonal trace sequence were manually aligned, allowing visualization of the indel patterns of each allele of a particular clone. In addition, whole-cell populations of CD34+ cells 72 hr post-transfection were analyzed by TIDE before clonal expansion and selection.

Statistical Analysis

For statistical comparisons among groups, Student's t test was used where appropriate.

SUPPLEMENTAL INFORMATION

Supplemental Information includes three figures and two tables and can be found with this article online at https://doi.org/10.1016/j.omtn.2018.01.013.

AUTHOR CONTRIBUTIONS

S.R.M., D.M., and N.R.-T. carried out the experiments. K.B. did the genetic analyses. P.B. and E.B.K. conceived the project. S.R.M. and E.B.K. wrote the manuscript.

CONFLICTS OF INTEREST

All authors declare that they have no competing interests.

ACKNOWLEDGMENTS

REFERENCES

1. Woolf, T.M., Gurumurthy, C.B., Boyce, F., and Kmiec, E.B. (2017). To cleave or not to cleave: therapeutic gene editing with and without programmable nucleases. Nat. Rev. Drug Discov. 16, 296.

2. Dever, D.P., Bak, R.O., Reinisch, A., Camarena, J., Washington, G., Nicolas, C.E., Pavel-Dinu, M., Saxena, N., Wilkens, A.B., Mantri, S., et al. (2016). CRISPR/Cas9 β-globin gene targeting in human haematopoietic stem cells. Nature 539, 384–389.

3. Xu, P., Tong, Y., Liu, X.Z., Wang, T.T., Cheng, L., Wang, B.Y., Lv, X., Huang, Y., and Liu, D.P. (2015). Both TALENs and CRISPR/Cas9 directly target the HBB IVS2-654 (C > T) mutation in β-thalassemia-derived iPSCs. Sci. Rep. 5, 12065.

4. Hendriks, W.T., Jiang, X., Daheron, L., and Cowan, C.A. (2015). TALEN- and CRISPR/Cas9-mediated gene editing in human pluripotent stem cells using lipid-based transfection. Curr. Protoc. Stem Cell Biol. 34, 5B.3.1–5B.3.25.

5. Liang, Q., Huashan, L., Yunhan, J., and Chunsheng, D. (2015). The molecular mechanism of CRISPR/Cas9 system and its application in gene therapy of human diseases. Yi Chuan *37*, 974–982.

6. Gundry, M.C., Brunetti, L., Lin, A., Mayle, A.E., Kitano, A., Wagner, D., Hsu, J.I., Hoegenauer, K.A., Rooney, C.M., Goodell, M.A., and Nakada, D. (2016). Highly efficient genome editing of murine and human hematopoietic progenitor cells by CRISPR/Cas9. Cell Rep. *17*, 1453–1461.

7. Richardson, C.D., Ray, G.J., DeWitt, M.A., Curie, G.L., and Corn, J.E. (2016). Enhancing homology-directed genome editing by catalytically active and inactive CRISPR-Cas9 using asymmetric donor DNA. Nat. Biotechnol. *34*, 339–344.

8. Doudna, J.A., and Charpentier, E. (2014). Genome editing. The new frontier of genome engineering with CRISPR-Cas9. Science *346*, 1258096.

9. Fellmann, C., Gowen, B.G., Lin, P.-C., Doudna, J.A., and Corn, J.E. (2017). Cornerstones of CRISPR-Cas in drug discovery and therapy. Nat. Rev. Drug Discov. *16*, 89–100.

10. Parekh-Olmedo, H., and Kmiec, E.B. (2007). Progress and prospects: targeted gene alteration (TGA). Gene Ther. *14*, 1675–1680.

11. Olsen, P.A., Randol, M., and Krauss, S. (2005). Implications of cell cycle progression on functional sequence correction by short single-stranded DNA oligonucleotides. Gene Ther. *12*, 546–551.

12. Olsen, P.A., Randøl, M., Luna, L., Brown, T., and Krauss, S. (2005). Genomic sequence correction by single-stranded DNA oligonucleotides: role of DNA synthesis and chemical modifications of the oligonucleotide ends. J. Gene Med. *7*, 1534–1544.

13. Radecke, S., Radecke, F., Peter, I., and Schwarz, K. (2006). Physical incorporation of a single-stranded oligodeoxynucleotide during targeted repair of a human chromosomal locus. J. Gene Med. *8*, 217–228.

14. Dekker, M., Brouwers, C., Aarts, M., van der Torre, J., de Vries, S., van de Vrugt, H., and te Riele, H. (2006). Effective oligonucleotide-mediated gene disruption in ES cells lacking the mismatch repair protein MSH3. Gene Ther. *13*, 686–694.

15. Ferrara, L., Engstrom, J.U., Schwartz, T., Parekh-Olmedo, H., and Kmiec, E.B. (2007). Recovery of cell cycle delay following targeted gene repair by oligonucleotides. DNA Repair (Amst.) *6*, 1529–1535.

16. Engstrom, J.U., Suzuki, T., and Kmiec, E.B. (2009). Regulation of targeted gene repair by intrinsic cellular processes. BioEssays *31*, 159–168.

17. Rios, X., Briggs, A.W., Christodoulou, D., Gorham, J.M., Seidman, J.G., and Church, G.M. (2012). Stable gene targeting in human cells using single-strand oligonucleotides with modified bases. PLoS ONE *7*, e36697.

18. Rivera-Torres, N., Banas, K., Bialk, P., Bloh, K.M., and Kmiec, E.B. (2017). Insertional mutagenesis by CRISPR/Cas9 ribonucleoprotein gene editing in cells targeted for point mutation repair directed by short single-stranded DNA oligonucleotides. PLoS One *12*, e0169350.

19. Strouse, B., Bialk, P., Niamat, R.A., Rivera-Torres, N., and Kmiec, E.B. (2014). Combinatorial gene editing in mammalian cells using ssODNs and TALENs. Sci. Rep. *4*, 3791.

20. Bialk, P., Rivera-Torres, N., Strouse, B., and Kmiec, E.B. (2015). Regulation of gene editing activity directed by single-stranded oligonucleotides and CRISPR/Cas9 systems. PLoS ONE *10*, e0129308.

21. Brinkman, E.K., Chen, T., Amendola, M., and van Steensel, B. (2014). Easy quantitative assessment of genome editing by sequence trace decomposition. Nucleic Acids Res. *42*, e168.

22. Bialk, P., Sansbury, B., Rivera-Torres, N., Bloh, K., Man, D., and Kmiec, E.B. (2016). Analyses of point mutation repair and allelic heterogeneity generated by CRISPR/Cas9 and single-stranded DNA oligonucleotides. Sci. Rep. *6*, 32681.

23. Baron, F., Ruggeri, A., and Nagler, A. (2016). Methods of *ex vivo* expansion of human cord blood cells: challenges, successes and clinical implications. Expert Rev. Hematol. *9*, 297–314.

24. Yu, X., Gu, Z., Wang, Y., and Wang, H. (2013). New strategies in cord blood cells transplantation. Cell Biol. Int. *37*, 865–874.

25. Flores-Guzmán, P., Fernández-Sánchez, V., and Mayani, H. (2013). Concise review: *ex vivo* expansion of cord blood-derived hematopoietic stem and progenitor cells: basic principles, experimental approaches, and impact in regenerative medicine. Stem Cells Transl. Med. *2*, 830–838.

26. Delaney, C., Ratajczak, M.Z., and Laughlin, M.J. (2010). Strategies to enhance umbilical cord blood stem cell engraftment in adult patients. Expert Rev. Hematol. *3*, 273–283.

27. Hendel, A., Bak, R.O., Clark, J.T., Kennedy, A.B., Ryan, D.E., Roy, S., Steinfeld, I., Lunstad, B.D., Kaiser, R.J., Wilkens, A.B., et al. (2015). Chemically modified guide RNAs enhance CRISPR-Cas genome editing in human primary cells. Nat. Biotechnol. *33*, 985–989.

28. DeWitt, M.A., Magis, W., Bray, N.L., Wang, T., Berman, J.R., Urbinati, F., Heo, S.J., Mitros, T., Muñoz, D.P., Boffelli, D., et al. (2016). Selection-free genome editing of the sickle mutation in human adult hematopoietic stem/progenitor cells. Sci. Transl. Med. *8*, 360ra134.

29. Wen, J., Tao, W., Hao, S., and Zu, Y. (2017). Cellular function reinstitution of offspring red blood cells cloned from the sickle cell disease patient blood post CRISPR genome editing. J. Hematol. Oncol. *10*, 119.

30. Hoban, M.D., Cost, G.J., Mendel, M.C., Romero, Z., Kaufman, M.L., Joglekar, A.V., Ho, M., Lumaquin, D., Gray, D., Lill, G.R., et al. (2015). Correction of the sickle cell disease mutation in human hematopoietic stem/progenitor cells. Blood *125*, 2597–2604.

31. Traxler, E.A., Yao, Y., Wang, Y.-D., Woodard, K.J., Kurita, R., Nakamura, Y., Hughes, J.R., Hardison, R.C., Blobel, G.A., Li, C., and Weiss, M.J. (2016). A genome-editing strategy to treat β-hemoglobinopathies that recapitulates a mutation associated with a benign genetic condition. Nat. Med. *22*, 987–990.